INVESTIGATION OF HIGH-CYCLE FATIGUE OF CAST IRON WITH POROUS LAYER NEAR THRESHOLD ΔK_{th}

MINDAUGAS LEONAVIČIUS, GEDIMINAS PETRAITIS, ALGIMANTAS KRENEVIČIUS, MARIJONAS ŠUKŠTA, STANISLAV STUPAK*

Vilnius Gediminas Technical University, Dept of Strength of Materials, Saultekio al. 11, LT-10223 Vilnius 40, Lithuania

Received 2 December 2004, accepted 27 July 2005

Cast iron used in manufacturing transport facilities and mining equipment may be made layered with various compositions. The results of experimental-analytical investigation into cyclic bending strength of seminatural rectangular cross-section cast iron specimens with a 10–11 mm thick porous layer are presented. The stress ratio $r = -0.62$, while stress ranges from 70 to 280 MPa. The bending specimens were tested under a great number of loading cycles – 3×10^8 (specimen 1) and 2×10^8 (specimen 2). Up to 1×10^8 cycles cracks propagated only in the surface porous layer. Then the main crack has formed and propagated into depth. The dependences of crack propagation rates on stress intensity factor were established. The presented results show that transitional layer arrests crack propagation, when crack front passes from porous to basic metal. The thresholds of discrete layers were established by testing CT specimens. It has been concluded that crack propagation character and the range of stress intensity factor threshold ΔK_{th} depend on the structure of the layer.

K e y w o r d s: cast iron, dross layer, structure, crack, fatigue, threshold

1. Introduction

The strength of any material used for structural elements depends on its mechanical and physical properties, which they acquire during one or more manufacturing processes. Cast iron with globular graphite is used for manufacturing transport and mining machinery [1, 2, 3]. Cast iron producing technology may be such that the produced cast iron can get a functional feature – to resist friction and cyclic loading (number of loading cycles $10^7 \leq N \leq 10^9$). This is typical of two- or three-

*corresponding author, e-mail: stupakas@adm.vtu.lt

-layered cast iron with different microstructures. The shape of fatigue cracks and their propagation has a great influence on the longevity of materials with these structures [4–6]. The main principles of fracture mechanics may be used in calculations [4, 7]. Some research has been carried out in this field [8]; however, the available knowledge is not sufficient when the number of cycles exceeds 10^8.

The well-known cast iron GGG-50 (DIN) was purposely manufactured with a porous layer, which improves its antifriction characteristics and resistance to cyclic loading. The experiments of cyclic strength determination by static and cyclic loading tests have been performed in the Laboratory of Strength Mechanics of Vilnius Gediminas Technical University. Testing conditions were close to actual working conditions of mineral grinding mills.

2. Experimental and analytical study

Cast iron foundrymen depend on key processing steps to achieve the desired microstructure of cast iron. The addition of Mg to cast iron is an essential processing step for manufacturing cast iron. Magnesium, a nodulizing agent, allows graphite to precipitate and grow in a nodular shape. Figure 1a shows the structure that was identified in the basic metal. It contains nodular graphite in the pearlitic matrix and ferrite surrounding graphite. The flake graphite developed in the transitional layer is shown in Fig. 1b.

In the surface layer structure (Fig. 1c) the graphite is in the shape of plates. The structures with plate graphite in the surface layer occur in ductile iron as the consequence of surface reactions with contaminants in the sand, usually sulphur, and they may become even more pronounced, depending on the Mg content versus the contaminant level in the sand. High contaminant and/or low Mg produce plates. Magnesium, however, is a highly reactive element. As a result, ductile iron often forms slag. The resulting reaction products are usually referred to as dross. The presence of Mg in molten iron also causes iron to generate slag. Dross results from the reaction of Mg with oxygen. When etched, the areas associated with dross will often have a ferritic structure. Dross-type structures can also be present if the metal is poured too cold. Sometimes the dross is associated with undissolved or partially dissolved inoculant. Another reason for the observed structures may be the presence of high-sulphur base iron contaminated with deleterious trace elements [9]. These formations impair the mechanical properties of cast iron. Specially produced layered cast iron should meet the particular usage requirements. Figure 1d shows structure of porous layer similar to that presented in Fig. 1c. The graphite is in the form of plates and flakes.

The mechanical properties of specimens taken from some layers were found as follows: porous layer (thickness 10–11 mm) $\sigma_{\mathrm{pr}} = 150$ MPa, $\sigma_{0.2} = 221$ MPa, $\sigma_{\mathrm{u}} = 225$ MPa, $E = 145$ GPa, $\delta \leq 1$ %, $\psi \leq 1$ %, basic metal (thickness ≈ 20 mm) $\sigma_{\mathrm{pr}} = 228$ MPa, $\sigma_{0.2} = 328$ MPa, $\sigma_{\mathrm{u}} = 507$ MPa, $E = 177$ GPa, $\delta = 3.8$ %,

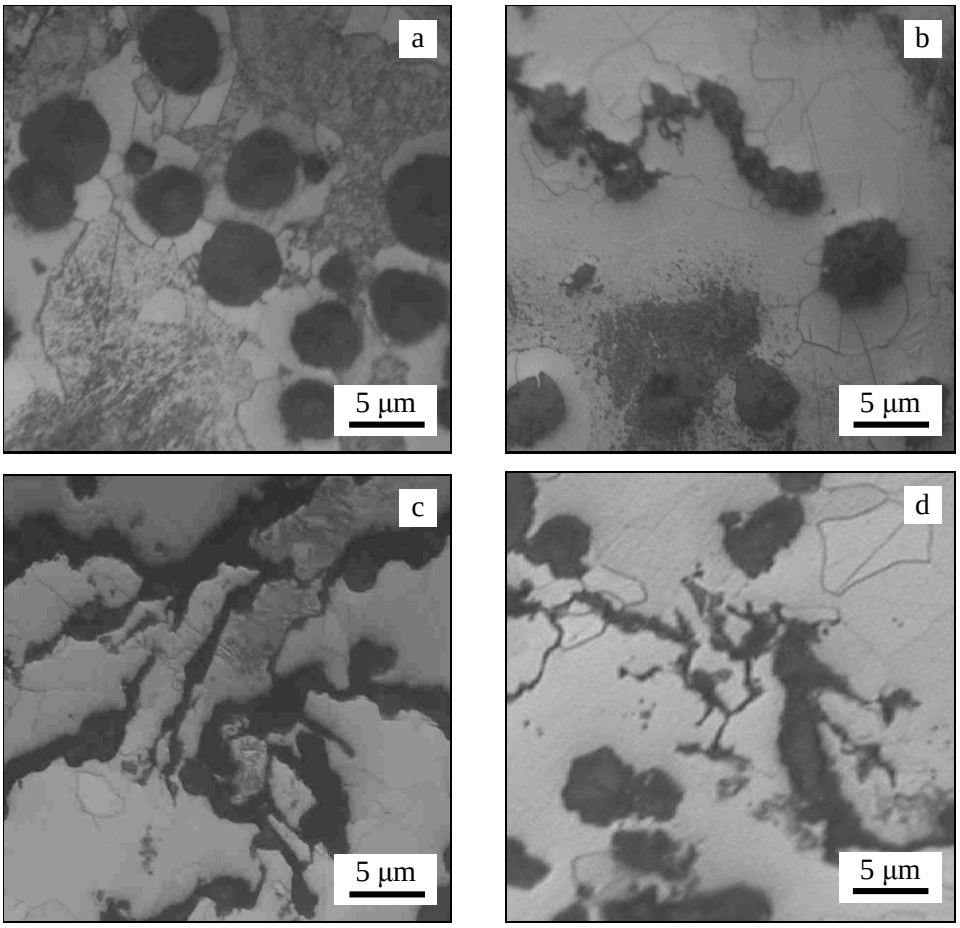

Fig. 1. Structure of the specimens (×200): a – basic metal, b – transitional layer, c – porous layer (specimen 1), d – porous layer (CT specimen).

ψ = 5.5 % and transitional layer (thickness ≈ 3 mm) σ_{pr} = 189 MPa, $\sigma_{0.2}$ = 275 MPa, σ_u = 366 MPa, E = 161 GPa, where σ_u is the ultimate tensile strength, σ_{pr} is the proportional limit, $\sigma_{0.2}$ is 0.2% offset yield strength, E is the Young's modulus, δ is the elongation, ψ is the reduction of the area.

The cyclic loading scheme of the specimen is shown in Fig. 2a. Rectangular cross-section specimens (Fig. 2b) were prepared using the same manufacturing technology as that applied in making actual structures. Stresses during experiments have been calculated on the assumption that specimens are continuous and homogeneous.

According to the type of specimen's fracture the locations of layers and their

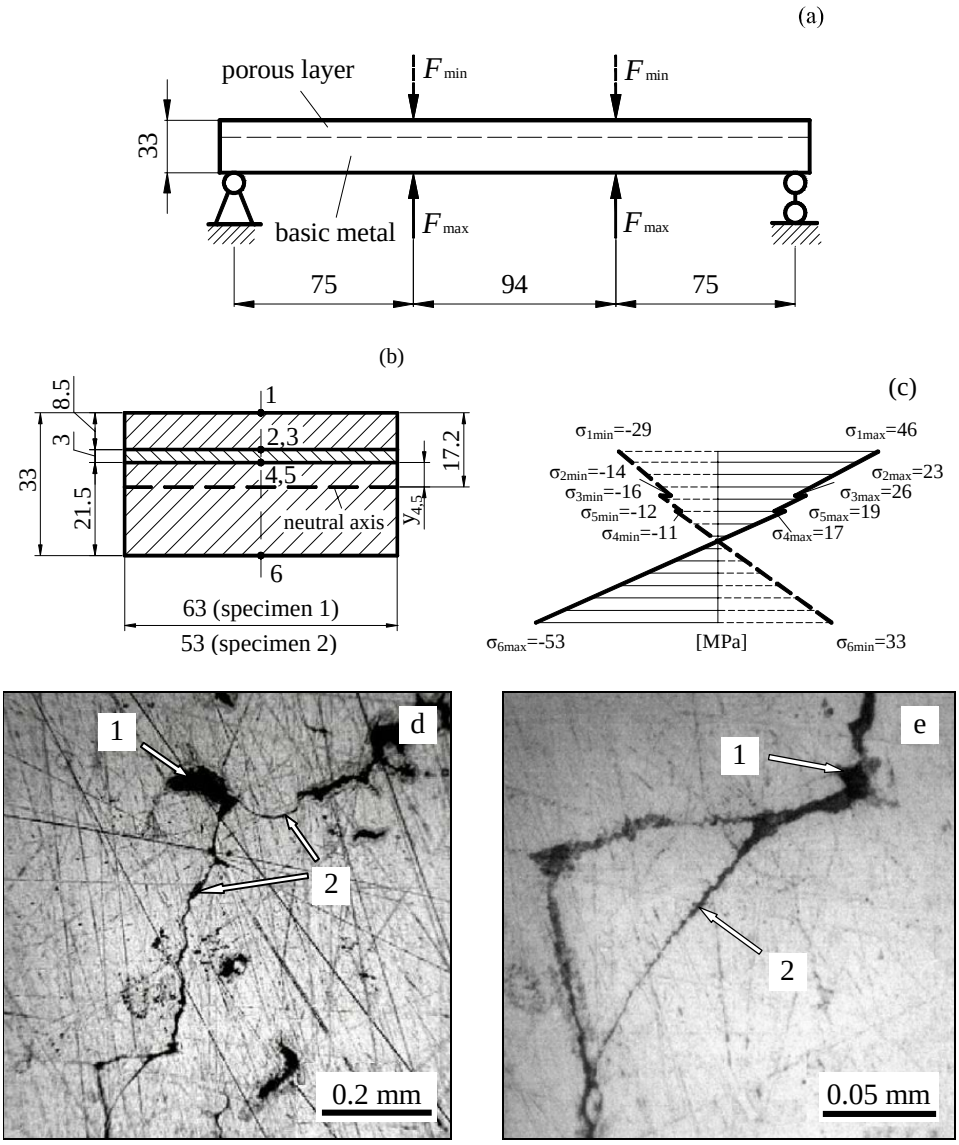

Fig. 2. Specimen's and loading data: loading scheme (a), cross-section (b), diagram of stresses (c), surface of porous layer (d), typical fragment of surface (e); 1 – graphite, 2 – crack.

dimensions were corrected (see Fig. 2b). In accordance with the hypothesis of plane sections, the normal stresses were calculated by equation:

$$\sigma_i = \frac{ME_i}{E_1 I_1 + E_2 I_2 + E_3 I_3} y_i, \tag{1}$$

where M is bending moment, I_i is inertia moment about the neutral axis, E_i is elasticity modulus of layer, y_i is distance from the point i to the neutral axis (Fig. 2b).

The stresses for specimen 1 (load case 1) are presented in Fig. 2c. The recalculated stresses of programmed loading are in Table 1.

Table 1. Specimen 1 stresses at points 1 . . . 6 (see Fig. 2)

Load case	Stresses according to $M_{\max}$ [MPa]						Stresses according to $M_{\min}$ [MPa]					
	σ_1	σ_2	σ_3	σ_4	σ_5	σ_6	σ_1	σ_2	σ_3	σ_4	σ_5	σ_6
1	46	23	26	17	19	−53	−29	−14	−16	−11	−12	33
2	59	30	33	22	24	−67	−37	−19	−20	−14	−15	42
3	73	37	41	27	29	−83	−45	−23	−25	−17	−18	51
4	93	47	52	34	37	−105	−58	−29	−32	−21	−23	65
5	100	51	56	37	41	−114	−62	−32	−35	−23	−25	71
6	106	54	60	39	43	−121	−66	−33	−37	−24	−27	75
7	114	57	64	42	46	−129	−71	−35	−40	−26	−29	80
8	120	61	68	44	49	−137	−74	−35	−42	−27	−30	85

For stress ratio $r = -0.62$, the stress ranges from $\Delta\sigma = 69$ MPa to $\Delta\sigma = 280$ MPa. The testing programme of cyclic loading was conducted in such a way that it is possible to identify crack formation and observe crack propagation in some layers applying non-destructive testing techniques (optical and luminescenic magnetic). The surface layer structure is prone to cracking, with cracks propagating in different directions. In Figs. 2d, 2e the surface of the specimen porous layer is shown. The main crack finally formed by joining together the neighbouring cracks when number of loading cycles is close to 10^8. Until 10^8 cycles the existing defects on the side surfaces of the specimens were growing negligibly. The extension of the stress range and the number of cycles increases the propagation of cracks on surface and the depth also becomes more significant. Specimen 1 disintegrated when stress alternating range reached 180 MPa. The total number of cycles was $N > 3 \times 10^8$. Specimen 2 has been statically broken, when the stress range reached 280 MPa. The total loading cycle is more than 2×10^8, taking into account the whole cyclic loading programme. In Figs. 3a and 3b the dependences of crack depth on stress range are shown including total fracture.

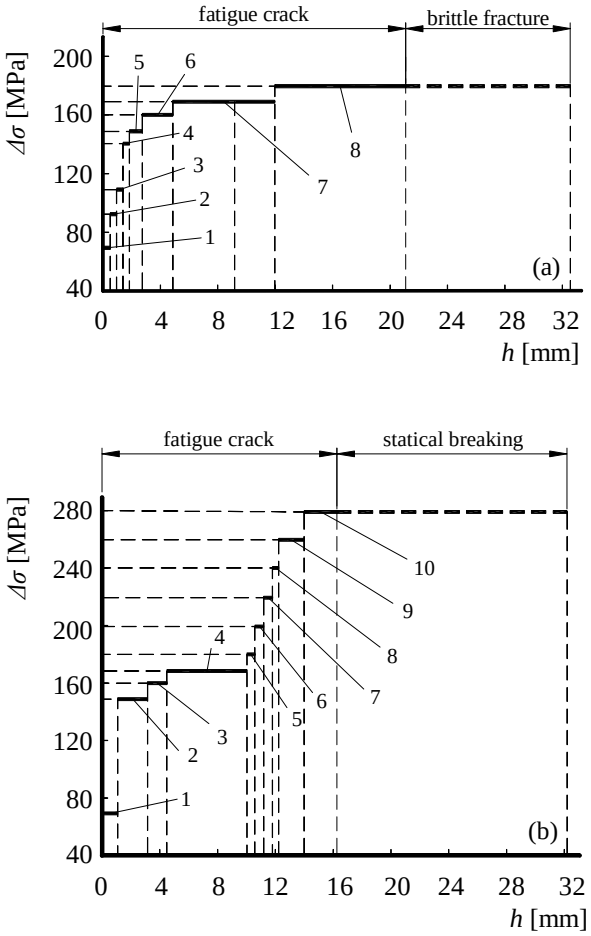

Fig. 3. Dependences of the crack depth on stress range: a – specimen 1, b – specimen 2 (1–10 – separate cases of programmed loading).

Transcrystalline spall dominated in fractures of specimens. It was also found that graphite globules exert a locally delaying effect on fatigue crack propagation. The tracks of programmed loading are noticeable. Structural formations of the porous layer are different, therefore the crack front in some locations enters the basic metal, while in others it is arrested in the porous layer or transitional layers. Durability of the specimen with a porous layer depends on the applied stresses and on the initial defect. In Figs. 4a, 4b the fractures of totally broken specimens are shown.

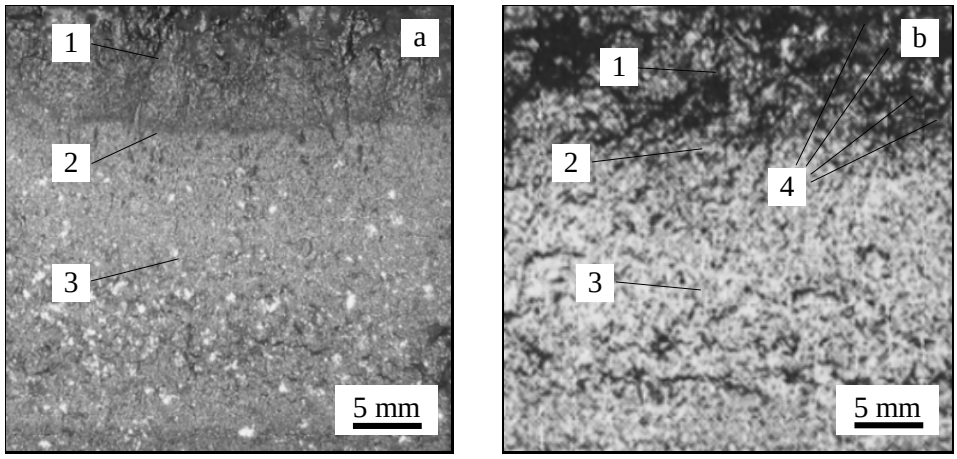

Fig. 4. Fractures surface of specimens: a – specimen 1, b – specimen 2 (1 – porous layer, 2 – transitional layer, 3 – basic metal, 4 – traces of programmed loading).

3. Crack propagation analysis

The assumption was made that crack propagation front is parallel to the specimen surface. Then the stress intensity factor K_{I} for rectangular cross-section specimen in pure bending can be calculated according to the formula

$$K_{\mathrm{I}} = \sigma\sqrt{\pi a} f(\alpha), \tag{2}$$

where σ is maximum tensile stress in the crack zone, a is crack length, $f(\alpha)$ – geometry function:

$$f(\alpha) = 1.122 - 1.40\alpha + 7.33\alpha^2 - 13.08\alpha^3 + 14.0\alpha^4, \tag{3}$$

where α is the ratio of the crack length a to the specimen width W.

Crack propagation rate versus the maximum stress intensity factor (according to the programmed loading) in three-layer plate is shown in Fig. 5a (specimen 1) and in Fig. 5b (specimen 2).

To determine the stress intensity range threshold ΔK_{th} the CT specimens were made of the basic metal and porous layer (their width $W = 42$ mm and thickness $B = 10$ mm). The dependences of crack growth rate versus the stress intensity factor range were determined (Fig. 6) meeting testing requirements and using the specified calculation technique (according to ASTM E 647-00 [10]). In the CT specimen made from basic metal, the crack plane was perpendicular to

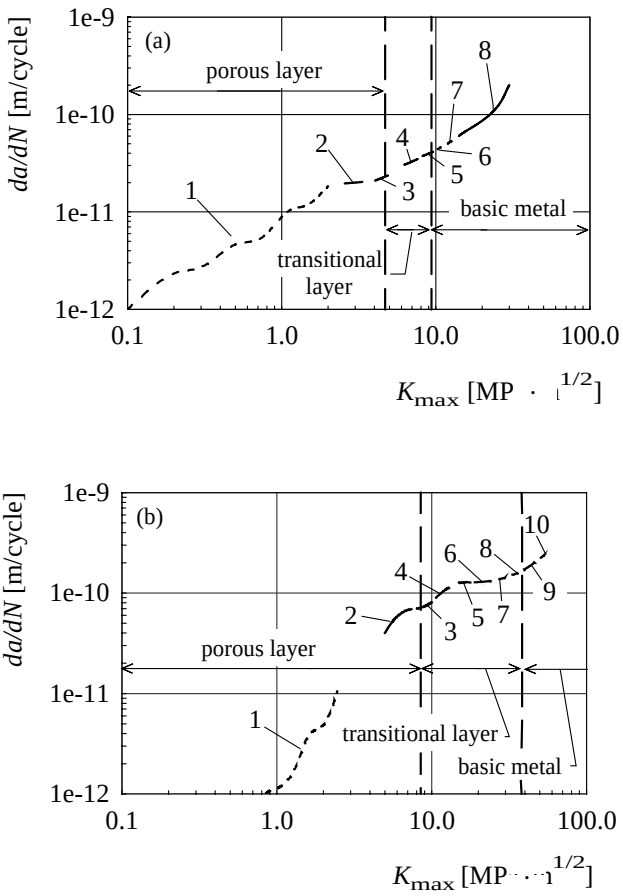

Fig. 5. Crack growth rate in plates versus the maximum stress intensity factor: a – specimen 1, b – specimen 2 (1–10 – number of program loading cases which are shown in Fig. 3).

bending normal stresses. The threshold of basic metal $\Delta K_{\mathrm{th}} = 9.3$ MPa$\cdot\sqrt{\mathrm{m}}$. In this specimen crack formation, propagation and arrest meet the well-known laws of fracture mechanics.

The threshold of porous layer $\Delta K_{\mathrm{th}}= 7.7$ MPa$\cdot\sqrt{\mathrm{m}}$. In the specimen made of a porous layer, crack formation and propagation depend on many factors. At the initial stage (crack depth 2–3 mm) a crack is formed in the area, which is under CT specimen notch (concentrator) influence and is almost perpendicular to normal stresses. The heterogeneity and anisotropy of separate layers of material have a great influence on further crack propagation. Cavities, heterogeneous

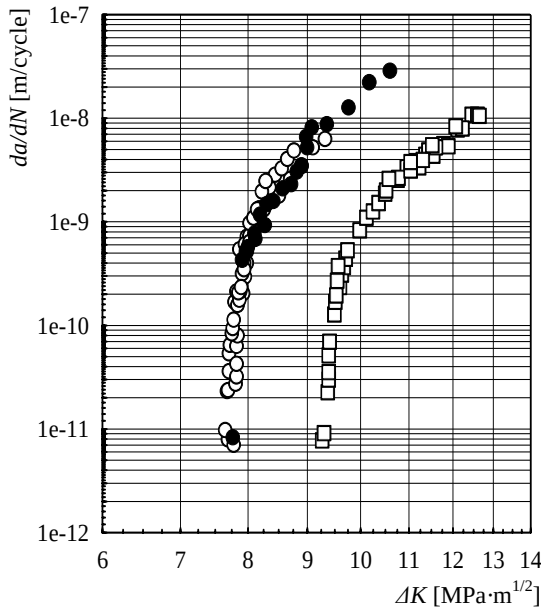

Fig. 6. Crack growth rate versus the stress intensity factor range (○, ● – porous layer, □ – basic metal).

formations and inserts change stress-strain state at the crack tip. The integral influence of structure on the separate segments determines the crack propagation so that its trajectory passes through slip planes and cavities in various directions. As shown in Fig. 7, on the sides of CT specimen, the crack not only changes its direction but splits into separate fronts. The crack bypasses separate inhomogeneous formations and cavities so that some macroparticles separate completely. Microstructural effects on the fatigue crack growth are found to be most significant in the near threshold regime (ΔK_{th}). This sensitivity seems to arise particularly as a result of crack front meeting with various structural particles involving at the same time opening and shear crack surface displacement modes. The loads can appear in sequential blocks, where one loading occurs in thousands of cycles and another only sporadically. This me-

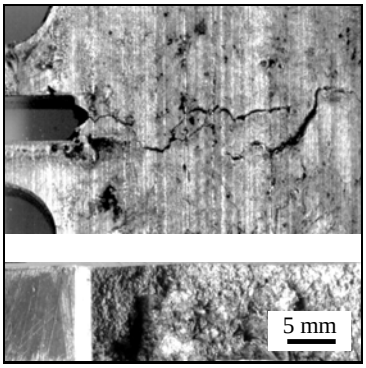

Fig. 7. Crack on specimen surface and fracture surface of CT specimen of porous layer.

chanism leads to zigzag crack propagation. Therefore the obtained porous layer's threshold ΔK_{th} is conditional, taking into account the assumption that a crack is perpendicular to normal bending stresses. It should be noted that obtained data are similar to two CT specimens of the porous layer.

4. Conclusions

1. It has been found that in the porous layer under high-cycle bending a great number of cracks are developed due to effect of cavities and heterogeneous formations.

2. When the range of cyclic stress is increased (according to programmed loading), the cracks propagate in various directions, but the main crack of irregular shape is formed depending both on external effects and layer's structure.

3. It has been found that the ultimate strength of basic metal ($\sigma_{\mathrm{u}} = 507$ MPa) is 2.2 times greater than that of the porous layer ($\sigma_{\mathrm{u}} = 225$ MPa). Basic metal threshold ($\Delta K_{\mathrm{th}} = 9.3\ \mathrm{MPa}\cdot\sqrt{\mathrm{m}}$) is 1.2 times greater than that of the porous layer ($\Delta K_{\mathrm{th}} = 7.7\ \mathrm{MPa}\cdot\sqrt{\mathrm{m}}$).

4. Great amounts of cavities, heterogeneous formations and plate graphite are found in the porous layer, and they influence crack propagation so that in some zones cracking enters basic metal, though in other locations it is arrested in the transitional layer.

5. Testing the CT specimens taken from the porous layer has shown that there simultaneously exist opening and shear crack surface displacement modes.

REFERENCES

[1] NADOT, Y.—MENDEZ, J.—RANGANATHAN, N.: I. J. Fatigue, *26*, 2004, p. 311.
[2] CALISTER, W. D.: Fundamentals of Materials Science and Engineering. New York, Wiley 2000.
[3] MARROW, T. J.—CENTINEL, H.—Al ZALMAH, M.: Fatigue & Fracture of Engineering & Structures, *25*, 2002, p. 635.
[4] MARROW, T. J.—CETINEL, H.—MACDONALD, S.—WITHERS, P. J.—VENSLOVAS, A.—LEONAVIČIUS, M.: In: Proceedings of the 14th Biennial Conference on Fracture – ECF14 – held in Cracow, Poland. Eds.: Neimitz, A. et al. Vol. II/III. Cracow, Poland, EMAS Publishing 2002, p. 443.
[5] HERTZBERG, R. W.: Deformation and Fracture Mechanics of Engineering Materials. New York, Wiley 1995.
[6] DORAZIL, E.: High Strength Austempered Ductile Cast Iron. Prague, Ellis Horwood 1991.
[7] ŽVINYS, J.: Structural Alloys. Cast Iron. Kaunas, Technologija 1999 (in Lithuanian).
[8] TROSHCHENKO, V.: Deformation and Fracture of Metals in High Cyclic Loading. Kijev, Naukova Dumka 1981 (in Russian).
[9] GOODRICH, G. M.: Explaining the Peculiar: Cast Iron Anomalies and Their Causes. Modern Casting, Schaumburg, AFS 1998.
[10] ASTM E 647-00. Standard Test Method for Measurement of Fatigue Crack Growth Rates, 2000.